

# Open Research Online

---

The Open University's repository of research publications and other research outputs

## Air-borne acoustic surface waves generated over a periodic rough surface

### Conference or Workshop Item

#### How to cite:

Stronach, Alexander; Bashir, Imran; Taherzadeh, Shahram and Attenborough, Keith (2016). Air-borne acoustic surface waves generated over a periodic rough surface. In: Proceedings of the Institute of Acoustics, 38(1) pp. 108–113.

For guidance on citations see [FAQs](#).

© [\[not recorded\]](#)

Version: Version of Record

---

Copyright and Moral Rights for the articles on this site are retained by the individual authors and/or other copyright owners. For more information on Open Research Online's data [policy](#) on reuse of materials please consult the policies page.

---

[oro.open.ac.uk](http://oro.open.ac.uk)

# AIR-BORNE ACOUSTIC SURFACE WAVES GENERATED OVER A PERIODIC ROUGH SURFACE

Alexander Stronach      School of Engineering & Innovation, The Open University, Milton Keynes  
Imran Bashir\*          School of Engineering & Innovation, The Open University, Milton Keynes  
Shahram Taherzadeh      School of Engineering & Innovation, The Open University, Milton Keynes  
Keith Attenborough      School of Engineering & Innovation, The Open University, Milton Keynes

\*Now at the University of Exeter.

## 1 INTRODUCTION

Although the generation of air-borne acoustic surface waves is a problem for noise control and measures must be taken to reduce their effect, surface waves can be used to passively amplify acoustic signals and thereby improve sensor performance.

Air-borne acoustic surface waves arise when a sound wave propagates over poroelastic or rough surface where the impedance has a greater reactance than resistance. Vertical to and fro motion of air particles due to sound penetrating the surface couples with the to and fro horizontal motion of air particles due to sound travelling parallel to the surface. The resultant elliptical motion is associated with a surface wave which traps sound energy at certain frequencies close to the surface resulting in an enhancement greater than the 6dB that would be associated with total reflection from an acoustically hard surface. They attenuate cylindrically with horizontal distance from the source and exponentially with height above the surface<sup>1</sup>.

Hutchinson-Howorth and Attenborough<sup>2</sup> carried out measurements over single and double lattice layers using tone bursts. They separated the surface wave contribution from the original impulse showing that the surface wave travels slower than the speed of sound in air.

Zhu et al<sup>3</sup> conducted measurements over a lattice and a mixed impedance ground surface, composed of strips, to investigate the passive amplification of signals through surface wave generation. It was found that a mixed impedance surface provided better amplification of acoustic signals than the lattice. Daigle & Stinson<sup>4</sup> also constructed a finite impedance surface using a strip of structured ground and found that the finite width of the strips gives rise to a directional response. This effect was exploited to obtain passive amplification and the sound pressure level found to be 6dB higher for sound travelling parallel to the strips compared to sound travelling transversely.

Bashir et al<sup>5</sup> carried out measurements over arrays of parallel rectangular aluminium strips to establish how strip-size and geometry affected the frequency content and magnitude of surface waves. The edge-to-edge spacing of the strips was varied between 0.003m and 0.006m. Frequency and time domain data shows that the surface wave shifts to lower frequencies as the mean spacing between the strips is increased. The magnitude was not found to change significantly. It was also found that the surfaces formed by the strips could be regarded as locally reacting rigid-framed hard-backed slit-pore layers with an effective depth slightly larger than the strip height when the spacing is close to the strip height. However, when the spacing is greater than the strip height, the surfaces behave as periodically rough surfaces.

The measurements conducted by Bashir et al indicates the possibility of more than one surface wave generated over the surface but so far have been interpreted as a consequence of the finite strip length. Surface wave generation by strips has been investigated through further measurements and the development of a Boundary Element Method (BEM) designed to study the surface waves in the time-domain.

## 2 MEASUREMENTS & SIMULATIONS

The measurements carried out by Imran Bashir et al<sup>5</sup> were conducted over periodically spaced rectangular aluminium strips placed over MDF. The strips have a height of 0.0253m and a width of 0.0126m and the source-receiver distance was varied between 0.7m and 1.3m. Measurements were carried out under anechoic conditions using a Tannoy® driver and a detachable 2m long Perspex tube, the end of which acts as a point source, and Bruel & Kjaer type 4311 0.5inch-diameter condenser microphone with a preamplifier as a receiver. The input signal used is a Maximum Length Sequence (MLS) impulse which has a high signal-to-noise ratio. The excess attenuation,  $EA$ , spectrum was then obtained using a free field,  $P_{free}$  measurement obtained by raising the microphone 2m above the floor of the anechoic chamber which minimises any unwanted reflections. The total field,  $P_{total}$ , was obtained by placing the source and receiver at 0.03m above the MDF surface (i.e 0.047m above the top of the strips). The excess attenuation can be calculated using equation Eq.(1),

$$EA = 20 \log \left( \frac{P_{total}}{P_{free}} \right) \quad (1)$$

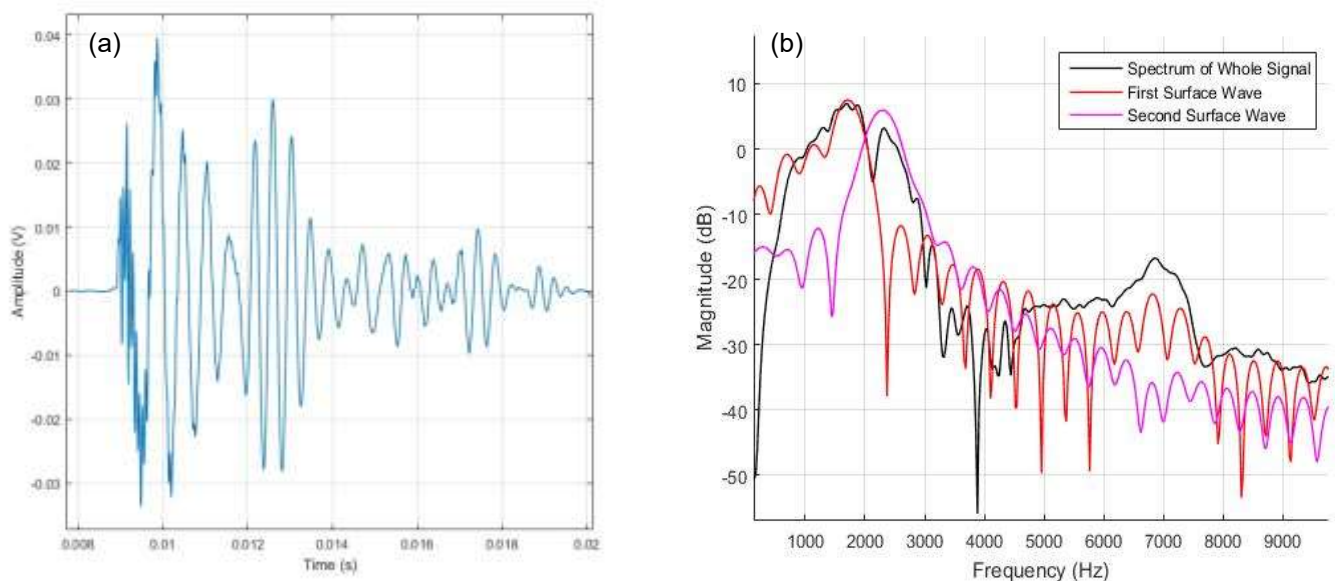


Figure 1(a): MLS pulse over rectangular strips with center-to-center spacing of 0.025m with source and receiver heights of 0.03m source-receiver distance 1m (b) Frequency spectrum obtained from a 4096-point FFT of the first and second surface wave components compared to the frequency spectrum of the entire signal.

Figure 1(a) shows time domain data and the corresponding frequency spectrum is shown in figure 1(b). In the frequency domain, the presence of a surface wave is indicated by a magnitude of greater than 6 dB (i.e. the maximum enhancement possible due to constructive interference from total reflection off the ground surface). In the time-domain, due its speed being slower than that of sound in air, the surface wave can be viewed as a separate arrival from the original impulse.

The frequency spectra show two distinct peaks around 2 kHz very close in frequency. A half-Blackman-Harris window was applied to the whole time-signal and a FFT of each time-interval

containing the surface waves was calculated. The two peaks in the frequency spectrum of the whole signal correspond to the frequencies obtained for each surface wave individually.

The time domain data show two distinctly separate arrivals, thus indicating that the two surface wave components have different speeds. One of the components follows almost immediately after the original impulse whereas the other arrives at the receiver later. This observation indicates that the first surface wave is travelling close to the speed of sound in air whereas the second travels slower.

## 2.1 TIME-DOMAIN BOUNDARY ELEMENT METHOD SIMULATIONS

The boundary element method is a numerical computational technique for solving partial differential equations formulated as boundary integrals. Solutions can be found at any point through the implementation of boundary conditions, which can be used to find the field at any point within a specified domain of interest. Taherzadeh et al<sup>6</sup> developed a 2-D BEM program in FORTRAN which predicts sound propagation above an uneven boundary.

The Boundary Element Method solves the field equations in the frequency domain. The software developed by Taherzadeh et al calculates excess attenuation data relative to the free field. The speeds of the potential surface wave components, however, are best investigated in the time domain. Thus, a BEM program has been developed calculates the sound field including the surface wave component in the time-domain.

The source function,  $S(\omega)$ , is an impulse or continuous noise. The frequency spectrum of the source signal is obtained using a Fast Fourier Transform (FFT). The response in the time-domain will be the Fourier integral of the product of the source function with the transfer function,  $p(r, z, \omega)$ , obtained from the BEM simulation:

$$p(r, z, t) = \frac{1}{2\pi} \int_{-f_{nyq}}^{f_{nyq}} S(\omega) p(r, z, \omega) e^{-i\omega t} d\omega \quad (2)$$

where the maximum frequency  $f_{nyq} = f_s/2$  and  $f_s$  is the sampling frequency. In order to account for the fact that it is not possible to integrate over negative frequencies, the fact that the solution to the Helmholtz wave equation is conjugate symmetric is used,

$$p(r, z, -\omega) = \overline{p(r, z, \omega)} \quad (3)$$

This allows for the Inverse Fast Fourier Transform (IFFT) to be taken for the full spectrum which yields the time-domain response.

The impedance model for surfaces used in these simulations is the Slit-Pore model developed by Attenborough<sup>7,8</sup>, since strips can be considered to act as a locally reacting rigid porous material composed of slit-like pores. The model yields expressions for complex density  $\rho_s(\omega)$ , complex compressibility  $C_s(\omega)$ , propagation constant  $k$  and characteristic impedance  $Z$  given by

$$\rho_s(\omega) = \frac{\rho_o}{1 - (\lambda_s \sqrt{-i})^{-1} \tanh(\lambda_s \sqrt{-i})}, \quad C_s(\omega) = (\gamma P_o)^{-1} \left( 1 + \frac{(\gamma - 1)}{\sqrt{-i N_{pr} \lambda_s}} \tanh(\sqrt{-i N_{pr} \lambda_s}) \right), \quad \lambda_s = \sqrt{\frac{3\omega \rho_o T}{\Omega R_s}} \quad (4a)$$

$$k = \omega \sqrt{T \rho(\omega) C(\omega)}, \quad Z = \frac{1}{\rho_o c_o} \sqrt{\frac{T}{\Omega^2} \frac{\rho(\omega)}{C(\omega)}} \quad (4b)$$

where  $\Omega$  is porosity,  $R_s$  is flow resistivity,  $T$  is tortuosity,  $\gamma$  is the ratio of specific heats,  $P_o$  is static atmospheric pressure,  $N_{pr}$  is the Prandtl number and  $\omega = 2\pi f$ .

The simulations were run with a source-receiver separation of 1m and 2m and a center-to-center spacing between the strips of 0.025m. The surface upon which the strips were placed was assumed to have  $R_s = 5 \times 10^6 \text{ Pa s m}^{-2}$  and  $\Omega = 0.01$  and the strips were assumed to be acoustically rigid.

The simulation results in figure 3 were conducted for a 1m source-receiver separation, as in the measurements. There is a distinct beat pattern present in figure 3(a) suggesting interference between two waves of slightly different frequency. The frequency spectra in figure 3(b) confirm that this is not simply a beat but, potentially, surface waves since there are peaks at 2 distinct frequencies. These spectra were obtained by windowing the first surface wave between 1ms and 3.5ms and the second surface wave between 3.5ms and 8ms. The primary surface wave seems to travel at close to the speed of sound in air, due to its immediate arrival after the original input pulse, whereas the second surface wave appears to travel slower. There is good agreement between the surface wave frequencies predicted by the BEM simulations and the frequencies obtained from the FFT of the time-domain data, indicating that the peaks observed in the excess attenuation spectra are indeed surface waves and not simply numerical artefacts.

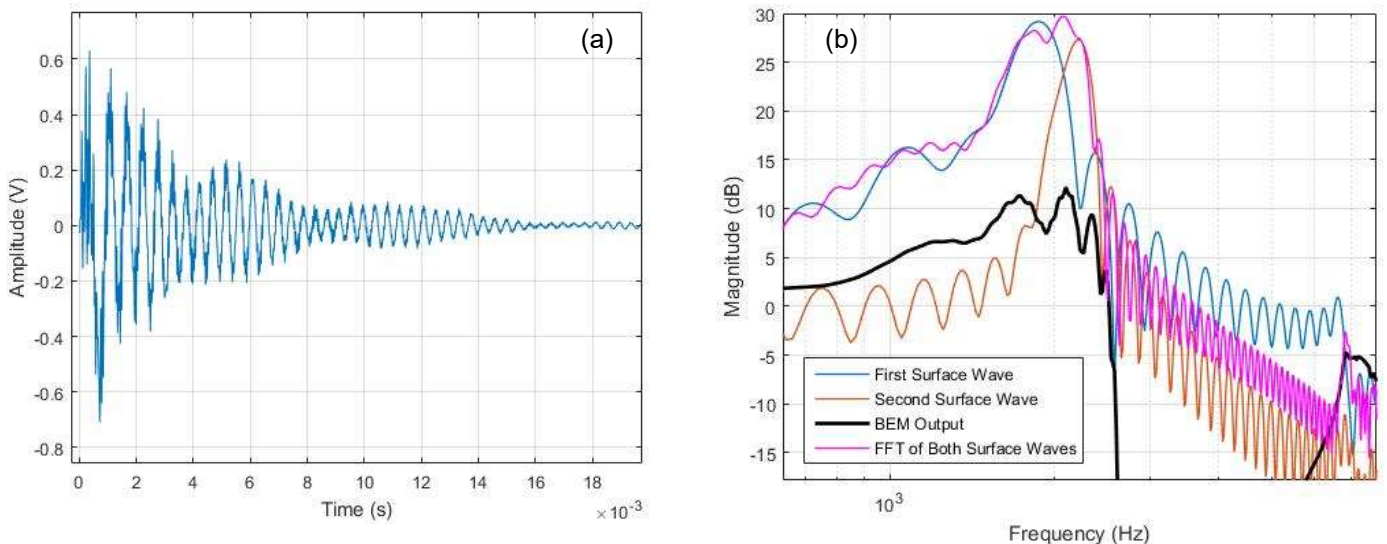


Figure 3: (a) Output from time-domain BEM with source-receiver separation of 1 m and strips with center-to-center spacing of 0.025 m. (b) Corresponding frequency spectra and excess attenuation from BEM output. The signal has been windowed to include the first surface wave only, the second surface wave only and both surface waves.

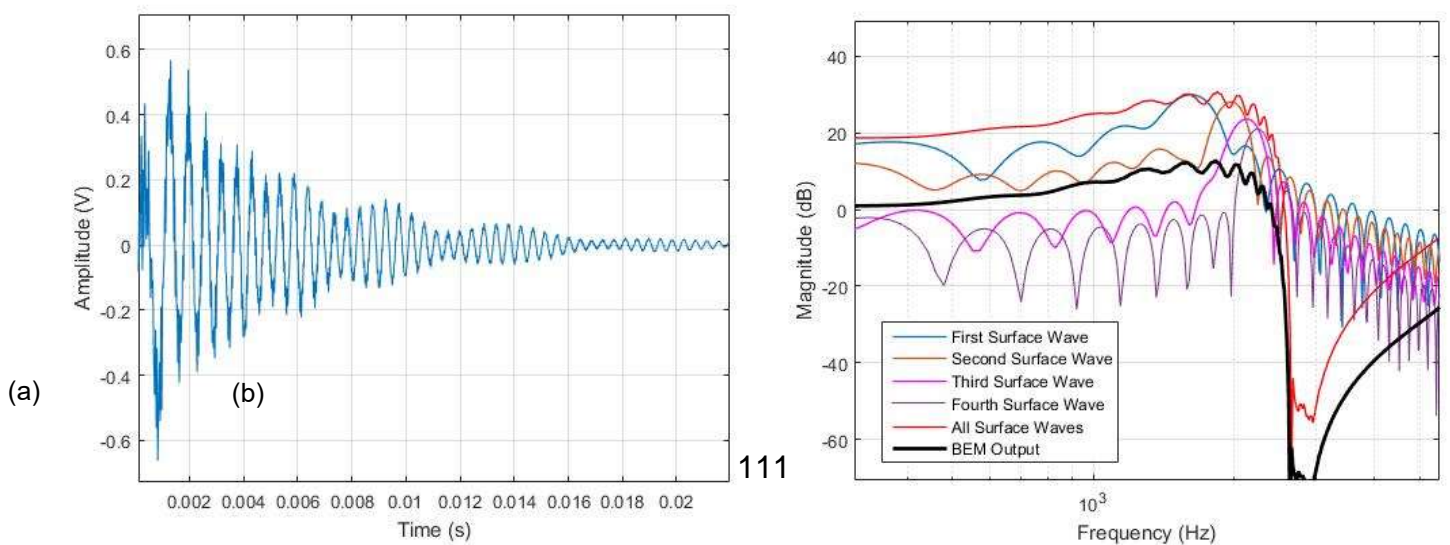


Figure 4 shows the output for a source-receiver separation of 2 m. Figure 4(a) shows more beats than the when the source-receiver separation was 1 m. This is due to the more complex pattern observed in the output of the BEM simulations. There is a possibility that the increased distance gives more time for acoustic energy to couple to surface waves at more frequencies. Again, the excess attenuation spectrum shows four distinct peaks at different frequencies and these frequencies correspond to the frequencies of distinct wave trains evident at the time domain plot. However, in figure 3(a), the first wave train occurs around 4 ms and this is the same in figure 4(a). The relative arrival time of the surface waves and the speed does not appear to change with increasing source-receiver distance.

### 3 CONCLUSIONS

Surface waves generated above rough surfaces composed of periodically spaced rectangular aluminium strips have been observed in the time- and frequency domain. Measurements conducted under anechoic conditions show the potential existence of more than one surface wave for a given source-receiver geometry and strip configuration. This has been investigated through predictions using a numerical time domain Boundary Element Method.

Output from simulations show beat patterns in the time-domain that indicate multiple waves of slightly different frequency. When the source-receiver separation is increased, more peaks can be seen in the excess attenuation spectrum and an increased number of beats observed in the time-domain. However, the arrival time of these surface waves does not change suggesting that the primary surface wave is separating into different components – each with its own frequency. The primary surface wave travels close to the speed of sound in air whilst the other components travel slower.

Further work will involve identifying the properties of the multiple peaks and their origin. It may also be possible to manipulate the frequency content and magnitude of the surface waves based on the source-receiver geometry and the strip dimensions. This will be useful in the passive amplification of signals at different frequencies.

### 4 REFERENCES

1. G.A. Daigle, M.R Stinson, D.I. Havelock (1996), Experiments on Surface Waves Over a Model Impedance Plane Using Acoustical Pulses, *Journal of Acoustical Society of America*, vol **99** (4), p1993
2. C. Hutchinson-Howorth, K. Attenborough (1992), Model Experiments on Air-Coupled Surface Waves, *Journal of Acoustical Society of America*, vol **92** (4), p2431
3. W. Zhu, G.A. Daigle, M.R Stinson (2003), Experimental and Numerical Study of Air-Coupled Surface Waves Generated Above Strips of Finite Impedance, *Journal of Acoustical Society of America*, vol **114** (3), p1243
4. G.A Daigle, M.R Stinson (2004), Passive Amplification and Directivity from Air-Coupled Surface Waves Generated Above a Structured Ground, *Journal of Acoustical Society of America*, vol **115** (5), p1988 – 1992
5. I. Bashir, S. Taherzadeh and K. Attenborough (2013), Surface waves over periodically-spaced rectangular strips, *Journal of Acoustical Society of America*, vol **134** (6), p4691
6. S. Taherzadeh, K.M Li, K. Attenborough (2001), A Hybrid BIE/FFP Scheme for Predicting Barrier Efficiency Outdoors, *Journal of Acoustical Society of America*, vol **110** (2), p918

7. K. Attenborough, I. Bashir, S. Taherzadeh, Outdoor Ground Impedance Models, *Journal of Acoustical Society of America*, vol **129** (5), p2806
8. K. Attenborough, K.M Li, K. Horoshenkov (2007), *Predicting Outdoor Sound*, Taylor & Francis, Abingdon.